Optimizing number squeezing when splitting a mesoscopic condensate

Julian Grond,[1] Jörg Schmiedmayer,[2] and Ulrich Hohenester[1]

[1]*Institut für Physik, Karl-Franzens-Universität Graz, Universitätsplatz 5, 8010 Graz, Austria*
[2]*Atominstitut der Österreichischen Universitäten, TU-Wien, Stadionallee 2, 1020 Wien, Austria*
(Received 24 June 2008; revised manuscript received 22 September 2008; published 9 February 2009)

We optimize number squeezing when splitting a mesoscopic Bose-Einstein condensate. Applying optimal control theory to a realistic description of the condensate allowed us to identify a form of the splitting ramp, which drastically outperforms the adiabatic splitting. The results can be interpreted in terms of a generic two-mode model mapped onto a parametric harmonic oscillator. This optimal route to squeezing paves the way to a much longer phase coherence and atom interferometry close to the Heisenberg limit.

PACS number(s): 03.75.−b, 02.60.Pn, 37.25.+k, 81.16.Ta

Confined atom interferometers using Bose-Einstein condensates (BECs) offer new prospects for matter-wave interferometry [1] and precision measurements. Optical dipole traps [2], atom chips [3], and radio-frequency (rf) potentials [4,5] provide powerful tools, which enable coherent manipulation and interference as demonstrated in a series of recent experiments [6–11].

Atom interferometers based on BECs usually suffer from the nonlinearity originating from atom-atom interactions, which leads to phase diffusion [12]. A possible way out is to seek for narrow number distributions of the split condensate—i.e., squeezed states, which are very powerful in precision measurements [13–16]. This can be achieved by adiabatic splitting, where the nonlinear interaction favors narrow number distributions [8,11,17]. The disadvantage of this scheme is the long time needed for the splitting process, within which technical noise and additional phase diffusion might threaten the interferometer performance [18–20].

In this paper, we show that splitting protocols, based on optimal control theory (OCT), allow efficient number squeezing on a much shorter time scale and drastically outperform adiabatic splitting. We first investigate the OCT problem in the framework of a simple two-mode model, leading us to an intuitive interpretation of the control strategy. The predictions of the simple model are verified for a realistic experimental setting by applying OCT to the many-body problem within the framework of multiconfigurational time-dependent Hartree equations for bosons [MCTDHB(2)] [21]. The fringe visibility is significantly enhanced in the case of optimized splitting, which renders this scheme ideal for atom interferometry.

Splitting a Bose-Einstein condensate is achieved by changing the confinement potential smoothly from a single well to a double well, as schematically shown in the inset of Fig. 1. We will assume that the condensate wave function is modified only along a single spatial direction x. To describe properly the fragmentation of the BEC into two spatially separated condensates, we need at least two wave functions $\phi_{L,R}(x)$, which we will refer to as left and right *orbitals*, together with an additional part that describes how the atoms are distributed among these two orbitals. Close to the splitting point, where the two orbitals become spatially separated, the system can be approximately described by a generic two-mode model, characterized by the Hamiltonian [17,22]

$$\hat{H} = -\frac{2}{N}E_j\hat{J}_x + \frac{1}{2}E_c\hat{J}_z^2.$$ (1)

Here, the Josephson energy E_j, which is proportional to the energy overlap of the orbitals, accounts for tunneling, whereas the charging energy E_c accounts for the nonlinear coupling of the atoms. $\hat{J}_x$ and $\hat{J}_z$ are pseudospin operators associated with these couplings [17,22]: $\hat{J}_x$ promotes an atom from the left to the right well, or vice versa, and $\hat{J}_z$ measures the atom number difference between the two wells.

In experiments, E_j is controlled indirectly by variation of the confinement potential. Here we use E_j itself as a control
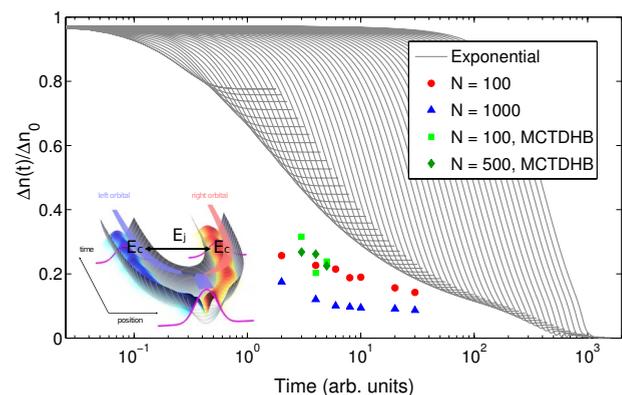

FIG. 1. (Color online) Time evolution of atom number fluctuations for $E_j(t)=E_j(0)\exp[-\frac{t}{\tau}]$ and for different decay constants τ, as computed within the generic two-mode model [17,22]. With increasing τ, the splitting process is more adiabatic and the fluctuations in the final state are lowered. The symbols report results of our OCT calculations for different numbers of atoms and splitting times T, and show that OCT can significantly outperform the more intuitive quasiadiabatic scheme for the exponential turning off. The square (diamond) symbols correspond to solutions obtained within MCTDHB for $N=100$ ($N=500$) (see Fig. 3). In the case of MCTDHB we take the E_c value after splitting for comparison. Inset: schematics of the BEC splitting process. By ramping up a double-well potential, the initial ground-state wave function of a single well becomes nonadiabatically split into two parts, denoted as left and right orbitals.

parameter, in order to grasp the essential features of the control strategy, and will lift this assumption later.

When tunneling dominates over the nonlinear interaction, $E_j \gg E_c N$, all atoms reside in the bonding orbital $\phi_g = \frac{1}{\sqrt{2}}(\phi_L + \phi_R)$, resulting in a binomial atom number distribution with fluctuation Δn_0. When the tunnel coupling is reduced, the nonlinear coupling favors localization of the atoms in one of the wells. The state of lowest energy is a superposition of different atom number states with smaller than binomial number fluctuations. In the limit of very small tunnel coupling, $E_j \rightarrow 0$, the ground state is such that half of the atoms reside in the left well and the other half in the right well, and there are no atom number fluctuations, $\Delta n = 0$.

To split the condensate, one starts from a state with $E_j \gg E_c N$ and then turns off the tunnel coupling. A quasiadiabatic splitting corresponds to an exponential decrease of E_j, as shown in Fig. 1 for different decay constants τ and 100–1000 atoms, corresponding to realistic experimental conditions. One observes that for slowly varying E_j the system evolves almost adiabatically and finally ends up in a state with small atom number fluctuations. For faster splitting, the system can no longer follow adiabatically and becomes frozen in a state with substantially larger number fluctuations (less number squeezing). By increasing τ by a factor of 10, the number fluctuations in the final state drop by a factor of approximately 2. *Thus, efficient atom number squeezing comes at the price of very slow splitting.*

To improve this we are seeking an optimal time variation of $E_j(t)$ that brings the system to a number squeezed state with reduced atom number fluctuations in much shorter time. To this end, we employ OCT [23–25] with the goal to minimize the atom number fluctuations $(\Delta n)^2$,

$$\mathcal{J} = (\Delta n)^2 = \langle \hat{J}_z^2 \rangle - \langle \hat{J}_z \rangle^2, \qquad (2)$$

in the state at the final time T. Within the framework of OCT, $\mathcal{J}$ is called the *cost function*, which is minimized under the constraint that the system's time evolution be governed by the Schrödinger equation. This is done by using Lagrange multipliers to turn the constrained minimization problem into an unconstrained one, as discussed in some length in Refs. [24,25].

Our OCT calculations within the two-mode model are summarized by the circular (for $N=100$) and triangular (for $N=1000$) symbols in Fig. 1. One clearly sees that the optimization of number squeezing works within a wide range of splitting times, and $E_j(t)$ sequences found in OCT perform approximately an order of magnitude faster in comparison to the standard exponential one.

Figure 2 shows details to one of the $E_j(t)$ time sequences of our squeezing optimization for $N=100$. OCT comes up with an oscillating tunnel control, which leads to a drastic reduction of the number fluctuations in comparison with the exponential turning off.

We next investigate why the oscillating OCT tunnel coupling drastically outperforms the more intuitive exponential decay. We show how to qualitatively understand the mechanism of the control.
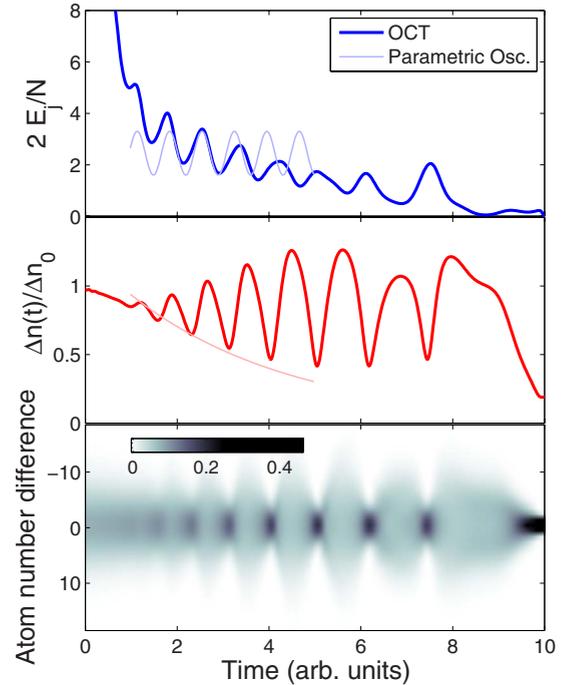

FIG. 2. (Color online) Results of OCT calculations for the generic two-mode model and for an atom number $N=100$. In (upper panel), we plot the tunneling control $E_j(t)$, in (middle panel) the time evolution of the atom number fluctuations, and in (lower panel) a density plot of the absolute square modulus of the atom number wave function. The bright lines show estimates based on the parametric oscillator of Eq. (4). The time interval has been chosen somewhat larger as in Fig. 3 to make the oscillating control mechanism more visible.

For large atom numbers N, the time evolution of the generic two-mode model can be approximately described by a harmonic oscillator [17]

$$i \dot{C}(k) = \left[-\frac{E_j}{2} \frac{\partial^2}{\partial k^2} + \left(\frac{2E_j}{N^2} + \frac{E_c}{2} \right) k^2 \right] C(k), \qquad (3)$$

where $C(k)$ is the atom-number wave function and k is the number difference between the left and right wells, which is treated as a continuous variable. Introducing the annihilation and creation operators $\hat{a}$ and $\hat{a}^\dagger$ for the harmonic oscillator [26], we can cast the Hamiltonian of Eq. (3) in the form

$$\hat{H} = 2 \widetilde{E}_j / N \left[\left(\hat{a}^\dagger \hat{a} + \frac{1}{2} \right) + \frac{E_c N^2}{16 \widetilde{E}_j} (\hat{a}^2 + \hat{a}^{\dagger 2}) \right]. \qquad (4)$$

Here $\widetilde{E}_j / N = E_j / N + E_c N / 8$ is the renormalized oscillator frequency. Equation (4) is the Hamiltonian for a parametric harmonic oscillator [27] with resonance frequency $\omega_{res} \approx 2E_j / N + E_c N / 4$.

When the oscillator is driven with approximately twice the resonance frequency, which is approximately the period of the OCT control in Fig. 2, the width of the initial ground-state wave packet starts to oscillate and becomes strongly squeezed. The predictions of the parametric oscillator model are plotted in Fig. 2 for the oscillating control field indicated
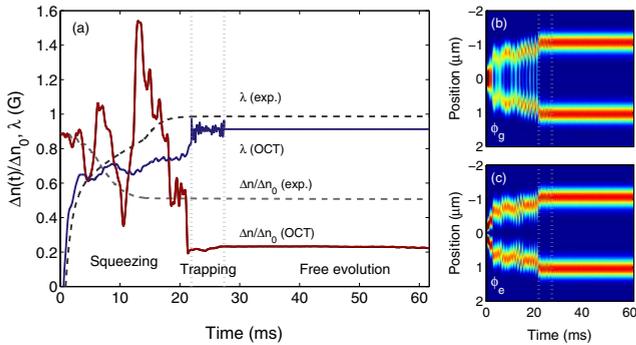
FIG. 3. (Color online) Optimized versus unoptimized splitting, as computed within MCTDHB(2). For the trap we use splitting by rf potentials [4], with $\omega_T = (2\pi) 2$ kHz transversal frequency, and the control field λ relates to the amplitude of the rf field $B_{rf} = (0.5 + 0.3\lambda)$ G. For an interaction strength [21] (chemical potential) of $g \approx 1.16$ Hz ($\mu \sim 2$ kHz for the unsplit trap), OCT improves squeezing considerably as compared to the exponential case. In the calculations we use *gerade* and *ungerade* orbitals $\phi_{g,e}$, rather than $\phi_{L,R}$, as they allow one to fully exploit the symmetry of the confinement potential. The scheme is quite robust to typical experimental noise of 30 μG (black lines, indistinguishable from OCT results). Panel (a) reports the control fields and atom number fluctuations for $N = 100$ for the exponential (dashed lines) and optimal control (solid lines), and panels (b) and (c) the time evolution of the *gerade* and *ungerade* orbitals.

in the upper panel: indeed, as can be observed from the number fluctuations in the middle panel, the envelope of $\Delta n(t)$ decreases in a fashion similar to the results of the OCT calculations. Thus, if we turn off E_j at the lower turning point of $\Delta n(T)$, we freeze the system in a squeezed number state [although the detailed freezing sequence of $E_j(t)$ happens to be more complex in the case of OCT].

We now address the question whether our findings would prevail in the case of a more realistic modeling of the many-body splitting process. Contrary to the two-mode model, where all details of the condensate orbitals are embodied in E_j and E_c, in general the control of E_j and E_c is indirect *through* the condensate orbitals, which, in turn, can be manipulated by means of the confinement potential $V_\lambda(x)$. Here, $\lambda(t)$ is a control parameter that describes the variation of the confinement potential when changing the external parameters, such as currents through the microtrap wires or frequency and strength of additional rf fields [4].

For a realistic description of the splitting process, we employ MCTDHB(2) [21], where the orbitals are determined self-consistently from a variational principle. This approach accounts in a natural manner for both the atom number fluctuations and the orbital dynamics. We raise the issue of whether the nonadiabatic dynamics of the orbitals allows us to exploit the same control mechanism as before.

In our calculations we use parameters typical for cigar-shaped potentials with a few 100–500 atoms, split along the transverse direction, similar to recent atom chip [6,7] or squeezing experiments [11] (see caption of Fig. 3 for details). We first choose $\lambda(t)$ such that the tunneling decays approximately monoexponentially. Figure 3 shows that for such

control the number fluctuations decay in a fashion similar to the generic two-mode model and the number squeezing in the final state is rather low.

Squeezing optimization is again performed within the framework of OCT [28]. Figure 3 shows the details of our OCT calculations. The density plot of the orbitals clearly shows that, as in the two-mode model calculation, the condensate is first brought to oscillations within the two wells, resulting in an oscillating tunnel coupling. In this regime the atom number fluctuations first oscillate wildly and then significantly drop. These results are in good agreement with the generic two-mode model; see Fig. 1.

To turn off the condensate oscillations after the squeezing optimization, we introduced an additional optimization step for the trapping of the orbitals, similar to our previous work on the optimization of the Gross-Pitaevskii equation [25]. With this, the orbitals are brought to an almost complete halt, as evidenced by the stationary evolution at later times [29].

We obtain similar results for larger atom numbers (500 atoms) and different splitting times. This makes us believe that the oscillating control for achieving a high degree of squeezing is of general nature and that the simple two-mode model provides a proper description for the underlying physics.

In the free-time evolution after splitting, an atom number superposition state with finite Δn undergoes a spread of evolution rates due to the nonlinear atom-atom interactions [12]. This "diffusion" of the relative phase with time degrades the coherence $\alpha := 2\text{Re}\langle \hat{a}_R^\dagger \hat{a}_L \rangle / N$ of the condensates, directly observable as the fringe contrast [30]. Here, $\hat{a}_L$ ($\hat{a}_R$) represents the mode operator for the left (right) condensate. To quantitatively analyze the improvement of OCT, we calculated the coherence 30 ms after splitting for $N = 100$ (500) atoms and found values of above 80% (90%) for OCT, to be contrasted with the values of close to zero (50%) for exponential splitting. *Thus our squeezing protocol strongly improves the phase coherence for a long time after splitting.*
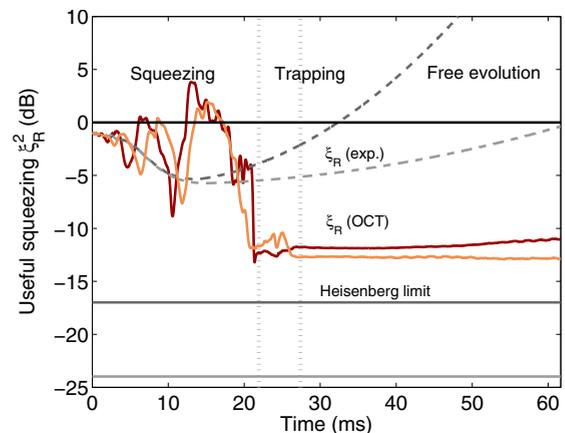

FIG. 4. (Color online) Useful squeezing ξ_R for $N = 100$ (dark lines) and $N = 500$ (bright lines) for the exponential (dashed lines) and optimal control (solid lines). The optimized solutions stay well beyond the standard quantum limit ($\xi_R = 1$), in sharp contrast to the unoptimized cases. The lines in the lower part indicate the Heisenberg limits $\xi_R = \sqrt{2/N}$ for the investigated N's.

Our OCT protocols will also be useful in experiments based upon the measurement of an atom number difference between the wells. The phase sensitivity is then quantified by the factor of *useful squeezing* $\xi_R = 2\Delta n / \sqrt{N}\alpha$ [14]. It displays that squeezing enhances the sensitivity below the shot-noise limit $\xi_R = 1$ and is (Heisenberg) limited from below by $\sqrt{2/N}$ [13]. Furthermore, $\xi_R < 1$ is a sufficient criterion for the presence of entanglement between the N atoms, signifying a type of entanglement, which is useful as a resource [11,31]. It is apparent from Fig. 4 that OCT squeezing achieves a phase sensitivity close to this fundamental limit of quantum measurements as well as the creation of N-body nonseparable states.

In conclusion, we have demonstrated that nonadiabatic condensate splitting following OCT allows for a very efficient number squeezing on short time scales, leading to a strongly enhanced phase coherence, thus rendering the technique powerful for interferometry applications.

[1] D. Cronin, J. Schmiedmayer, and D. E. Pritchard, e-print arXiv:0712.3703.

[2] R. Grimm, M. Weidemüller, and Y. Ovchinnikov, Adv. At., Mol., Opt. Phys. **42**, 95 (2000).

[3] R. Folman, P. Krüger, J. Schmiedmayer, J. Denschlag, and C. Henkel, Adv. At., Mol., Opt. Phys. **48**, 263 (2002).

[4] I. Lesanovsky, T. Schumm, S. Hofferberth, L. M. Andersson, P. Krüger, and J. Schmiedmayer, Phys. Rev. A **73**, 033619 (2006).

[5] S. Hofferberth, I. Lesanovsky, B. Fischer, J. Verdu, and J. Schmiedmayer, Nat. Phys. **2**, 710 (2006).

[6] T. Schumm, S. Hofferberth, L. M. Andersson, S. Wildermuth, S. Groth, I. Bar-Joseph, J. Schmiedmayer, and P. Krüger, Nat. Phys. **1**, 57 (2005).

[7] S. Hofferberth, I. Lesanovsky, B. Fischer, T. Schumm, and J. Schmiedmayer, Nature (London) **449**, 324 (2007).

[8] G.-B. Jo, Y. Shin, S. Will, T. A. Pasquini, M. Saba, W. Ketterle, D. E. Pritchard, M. Vengalattore, and M. Prentiss, Phys. Rev. Lett. **98**, 030407 (2007).

[9] S. Hofferberth, I. Lesanovsky, T. Schumm, A. Imambekov, V. Gritsev, E. Demler, and J. Schmiedmayer, Nat. Phys. **4**, 489 (2008).

[10] M. Albiez, R. Gati, J. Fölling, S. Hunsmann, M. Cristiani, and M. K. Oberthaler, Phys. Rev. Lett. **95**, 010402 (2005).

[11] J. Estève, C. Gross, A. Weller, S. Giovanazzi, and M. K. Oberthaler, Nature (London) **455**, 1216 (2008).

[12] J. Javanainen and M. Wilkens, Phys. Rev. Lett. **78**, 4675 (1997).

[13] V. Giovannetti, S. Lloyd, and L. Maccone, Science **306**, 1330 (2004).

[14] D. J. Wineland, J. J. Bollinger, W. M. Itano, and D. J. Heinzen, Phys. Rev. A **50**, 67 (1994).

[15] M. H. Schleier-Smith, I. D. Leroux, and V. Vuletic, e-print arXiv:0810.2582v1.

[16] J. Appel, P. J. Windpassinger, D. Oblak, U. B. Hoff, N. Kjaergaard, and E. S. Polzik, arXiv:0810.3545v1.

[17] J. Javanainen and M. Y. Ivanov, Phys. Rev. A **60**, 2351 (1999).

[18] A. A. Burkov, M. D. Lukin, and E. Demler, Phys. Rev. Lett. **98**, 200404 (2007).

[19] Y. Li, Y. Castin, and A. Sinatra, Phys. Rev. Lett. **100**, 210401 (2008).

[20] Y. Khodorkovsky, G. Kurizki, and A. Vardi, Phys. Rev. Lett. **100**, 220403 (2008).

[21] O. E. Alon, A. I. Streltsov, and L. S. Cederbaum, Phys. Rev. A **77**, 033613 (2008).

[22] G. J. Milburn, J. Corney, E. M. Wright, and D. F. Walls, Phys. Rev. A **55**, 4318 (1997).

[23] A. P. Peirce, M. A. Dahleh, and H. Rabitz, Phys. Rev. A **37**, 4950 (1988).

[24] A. Borzì, G. Stadler, and U. Hohenester, Phys. Rev. A **66**, 053811 (2002).

[25] U. Hohenester, P. K. Rekdal, A. Borzì, and J. Schmiedmayer, Phys. Rev. A **75**, 023602 (2007).

[26] A. Messiah, *Quantum Mechanics* (North-Holland, Amsterdam, 1965).

[27] M. O. Scully and M. S. Zubairy, *Quantum Optics* (Cambridge University Press, Cambridge, UK, 1997).

[28] We use an analogous cost functional as in the case of the simple two-mode model [Eq. (2)], but with the system constrained to the time evolution of the MCTDHB(2) equations. This results in a much more involved optimality system as compared to the former model. Details of the optimality system and our numerical implementation will be given elsewhere.

[29] Also, in the stage termed "squeezing" optimization, we used a cost functional comprised of both the number of fluctuations at the final time and terms accounting for the trapping of the orbitals.

[30] L. Pitaevskii and S. Stringari, Phys. Rev. Lett. **87**, 180402 (2001).

[31] A. Sorensen, L. M. Duan, J. I. Cirac, and P. Zoller, Nature (London) **409**, 63 (2001).